

Dissipation in dynamics of a moving contact line

Ramin Golestanian^{1,2,3} and Elie Raphaël¹

¹*Laboratoire de Physique de la Matière Condensée, Collège de France, URA No. 792 du CNRS, 11 place Marcelin-Berthelot, 75231 Paris Cedex 05, France*

²*Institute for Advanced Studies in Basic Sciences, Zanjan 45195-159, Iran*

³*Institute for Studies in Theoretical Physics and Mathematics, P.O. Box 19395-5531, Tehran, Iran*

(Received 29 March 2001; published 7 August 2001)

The dynamics of the deformations of a moving contact line is studied assuming two different dissipation mechanisms. It is shown that the characteristic relaxation time for a deformation of wavelength $2\pi/|k|$ of a contact line moving with velocity v is given as $\tau^{-1}(k) = c(v)|k|$. The velocity dependence of $c(v)$ is shown to depend drastically on the dissipation mechanism: we find $c(v) = c(v=0) - 2v$ for the case in which the dynamics is governed by microscopic jumps of single molecules at the tip (Blake mechanism), and $c(v) \approx c(v=0) - 4v$ when viscous hydrodynamic losses inside the moving liquid wedge dominate (de Gennes mechanism). We thus suggest that the debated dominant dissipation mechanism can be experimentally determined using relaxation measurements similar to the Ondarcuhu-Veyssie experiment [T. Ondarcuhu and M. Veyssie, *Nature* **352**, 418 (1991)].

DOI: 10.1103/PhysRevE.64.031601

PACS number(s): 68.03.-g, 68.08.-p, 05.40.-a

I. INTRODUCTION

Spreading of a liquid on a solid surface usually involves a rather complex dynamical behavior, which is determined by a subtle competition between the mutual interfacial energetics of the coexisting phases (the solid, the liquid, and the corresponding equilibrium vapor), dissipation processes, and geometrical or chemical irregularities of the solid surface [1]. Interestingly, this dynamics can be effectively studied in terms of the dynamics of the *contact line*, which is the common borderline between the three phases, by correctly taking into account the physical processes in the vicinity of it.

One of the key issues about this dynamics that has remained a subject of controversy is dissipation. There are two rival theories in the literature, each depicting a different physical picture for the dominant dissipation mechanism in the dynamics of partial wetting [2]. The first approach, which is based on the idea of Yarnold and Mason [3] and was later developed into a quantitative theory by Blake and co-workers [4], emphasizes the role of microscopic jumps of single molecules (from the liquid into the vapor) in the immediate vicinity of the contact line. The other approach, which was developed by de Gennes and co-workers [1,5], asserts that for small values of contact angle the dissipation is dominated by viscous hydrodynamic losses inside the moving liquid wedge.

For a partially wetting fluid on sufficiently smooth substrates, a contact line at equilibrium has a well-defined contact angle θ_e that is determined by the solid-vapor γ_{SV} and the solid-liquid γ_{SL} interfacial energies, and the liquid surface tension γ through Young's relation: $\gamma_{SV} - \gamma_{SL} = \gamma \cos \theta_e$. For a moving contact line, however, the value of the so-called dynamic contact angle θ_d changes as a function of velocity: $\theta_d > \theta_e$ for an advancing contact line and $\theta_d < \theta_e$ for a receding one. Since the discrepancy between the two dissipation mechanisms appears for small contact angles [2], one can expect that receding contact lines are in fact very good candidates for experimental determination of the domi-

nant mechanism in this regime.

A classic example of this corresponds to wetting of a plate that is vertically withdrawn from a liquid at a constant velocity $-v$, which was first studied by Landau and Levich for complete wetting [6]. In the case of partial wetting that was studied by de Gennes [5,7], a steady state is achieved in which the liquid will partially wet the plate with a nonvanishing dynamic contact angle $\theta_d(v)$ only for pull-out velocities less than a certain critical value v_c . The dynamic contact angle decreases with increasing v , until at the critical velocity the system undergoes a dynamical phase transition in which a macroscopic Landau-Levich liquid film, formally corresponding to a vanishing θ_d , will remain on the plate.

Since the onset of leaving a film occurs at small values of contact angle, one can imagine that the two different dissipation mechanisms would lead to conflicting predictions about the transition. In particular, in Blake's picture the "order parameter" for the transition θ_d would vanish continuously as v approaches v_c , which makes it look like a second-order phase transition. On the contrary, de Gennes predicts a jump in the order parameter from $\theta_e/\sqrt{3}$ to zero at the transition, which is the signature of a first-order phase transition [2,5]. This drastic difference in the predictions of the two theories can provide a reliable venue for testing them. However, such experiments have so far proven to be inconclusive due to the usual difficulties of tuning into a critical point in the presence of disorder [8].

Another notable feature of contact lines is their anomalous elasticity as noticed by Joanny and de Gennes [9]. For length scales below the capillary length (which is of the order of 3 mm for water at room temperature), a contact line deformation of wave vector k , denoted as $h(k)$ in Fourier space, will distort the surface of the liquid over a distance $|k|^{-1}$. Assuming that the surface deforms instantaneously in response to the contact line, the elastic energy cost for the deformation can be calculated from the surface tension energy stored in the distorted area, and is thus proportional to $|k|$, namely [9]

$$E_{cl} = \frac{\gamma\theta_e^2}{2} \int \frac{dk}{2\pi} |k| |h(k)|^2. \quad (1)$$

The anomalous elasticity leads to interesting equilibrium dynamics, corresponding to when the contact line is perturbed from its static position, as studied by de Gennes [10]. Balancing dE_{cl}/dt and the dissipation, which he assumes for small contact angles is dominated by the hydrodynamic dissipation in the liquid nearby the contact line, he finds that each deformation mode relaxes to equilibrium with a characteristic inverse decay time $\tau^{-1}(k) = c_0|k|$, in which $c_0 = \gamma\theta_e^3/(3\eta\ell)$, where η is the viscosity of the liquid and ℓ is a logarithmic factor of order unity [10]. The relaxation is thus characterized by a linear dispersion relation, which implies that a deformation in the contact line will decay and propagate at a constant velocity c_0 , as opposed to systems with normal line tension elasticity, where the decay and the propagation are governed by diffusion. This behavior has been observed, and the linear dispersion relation has been precisely tested, in a very interesting experiment by Ondarcuhu and Veyssie [11].

Here we study the dynamics of the deformations of a moving contact line for the two different dissipation mechanisms. In particular, we focus on the sizeable regime where the contact line is moving, i.e., it is away from the depinning transition [12], but still not too close to the onset of leaving a film. We show that in this regime, the characteristic relaxation time for a k -mode deformation is given as $\tau^{-1}(k) = c(v)|k|$. The velocity dependence of $c(v)$ is shown to depend drastically on the dissipation mechanism: we find $c(v) = c(v=0) - 2v$ in Blake's scheme, whereas in de Gennes' picture $c(v)$ might be rather well represented by $c(v) \approx c(v=0) - 4v$. We thus suggest that monitoring the deformation dynamics in this regime, along the lines of the Ondarcuhu-Veyssie experiment [11], can provide a more practical probe for the experimental determination of the debated dominant dissipation mechanism.

The rest of the paper is organized as follows. In Sec. II, we discuss the two different dissipation mechanisms and derive expressions for the corresponding energy dissipation rates. These expressions are then used in Sec. III to derive the force balance, and thus the governing dynamical equation. The velocity dependence of the dynamic contact angle and a characteristic velocity are studied in Secs. IV and V correspondingly. While Sec. VI discusses the effects of surface disorder, we conclude with some discussions in Sec. VII.

II. DISSIPATION

Let us assume that the contact line is directed on average along the x axis, and is moving in the y direction with an average velocity v , which we assume to be positive corresponding to receding contact lines, as in Fig. 1. We can describe the position of the contact line along the y axis for any given x and t with the function $y(x,t) = vt + h(x,t)$. We further assume that the deformation $h(x,t)$ is only a relatively small perturbation. We can now try to evaluate the overall

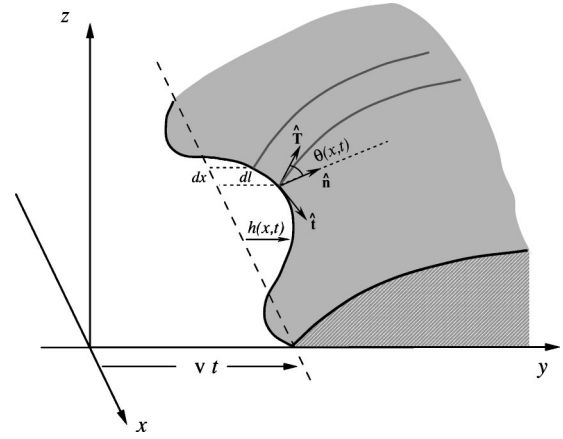


FIG. 1. The schematics of the system.

dissipation for the deforming contact line within the two different scenarios.

A. Blake approach

The physical process that is involved in causing dissipation in Blake's picture, i.e., molecular jumps near the contact line, is *local* in nature [4]. Therefore, in any small neighborhood the amount of dissipation is completely determined by the local value of the contact line velocity, while all the molecular details of the dissipation is encoded in an effective friction coefficient μ^{-1} . The overall dissipation can then be written as

$$P_l = \frac{1}{2\mu} \int dx [v + \partial_t h(x,t)]^2. \quad (2)$$

In the limit of relatively small contact angles, which is relevant for our receding contact lines, the inverse friction coefficient (or mobility) can be calculated as [2]

$$\mu = \frac{k\lambda^3}{k_B T} \exp\left(-\frac{W}{k_B T}\right), \quad (3)$$

in which W is an activation energy for molecular hopping, λ is the distance between hopping sites, k is a characteristic "attempt" rate, and $k_B T$ is the thermal energy.

B. de Gennes approach

We now focus on the contribution of dissipation that comes from the viscous losses in the hydrodynamic flows inside the liquid wedge [1,5]. For a slightly deformed contact line, we assume that the dissipation can be approximated by the sum of contributions from wedge-shaped slices with local contact angles $\theta(x,t)$, as shown in Fig. 1. This is a reasonable approximation because most of the dissipation is taking place in the singular flows near the tip of the wedge [1,5,10]. Using the result for the dissipation in a perfect wedge, which is based on the lubrication approximation [1,13], we can calculate the total dissipation as [10]

$$P_h = \frac{\eta}{2} \int dx \left(\frac{3\ell}{\theta(x,t)} \right) [v + \partial_t h(x,t)]^2, \quad (4)$$

in which $\ell = \ln(d_{\max}/d_{\min})$ with d_{\max} given by the size of the liquid drop and d_{\min} being a microscopic length scale. The inverse dependence on θ suggests that for sufficiently small contact angles the hydrodynamic loss is to be dominant [2].

III. FORCE BALANCE AND DYNAMICAL EQUATION

To find the governing dynamical equation in the long-time limit, we should balance the total friction force obtained as $\delta(P_l + P_h)/\delta\partial_t h(x,t)$ with the interfacial force $\gamma \cos \theta(x,t) - (\gamma_{SV} - \gamma_{SL}) = \gamma[\cos \theta(x,t) - \cos \theta_e]$ at each point along the contact line. Note that in this section, we are taking both dissipation mechanisms into account. In the limit of small contact angles, we find

$$\left[\frac{1}{\mu} + \frac{3\eta\ell}{\theta(x,t)} \right] [v + \partial_t h(x,t)] = \frac{\gamma}{2} [\theta_e^2 - \theta(x,t)^2]. \quad (5)$$

To proceed from here, we need to relate the contact angle $\theta(x,t)$ to the contact line profile $h(x,t)$, which can be done through solving for the surface profile of the liquid drop. One can show that the surface profile $z(x,y)$ near the contact line can be found as a solution of the Laplace equation $(\partial_x^2 + \partial_y^2)z(x,y) = 0$, so as to minimize the surface area. The solution that satisfies the boundary condition $z(x, h(x,t)) = 0$ reads [9]

$$z(x,y) = \theta_d \left[y - \int \frac{dk}{2\pi} h(k,t) e^{ikx - |k|y} \right], \quad (6)$$

from which we obtain

$$\theta(x,t) \equiv \left. \frac{\partial z(x,y)}{\partial y} \right|_{y=h(x,t)} = \theta_d \left[1 + \int \frac{dk}{2\pi} |k| h(k,t) e^{ikx} \right], \quad (7)$$

to the leading order [9].

To the zeroth order, Eq. (5) gives the relation between the average dynamic contact angle and the velocity as

$$v = \left(\frac{\gamma}{6\eta\ell} \right) \frac{\theta_d(\theta_e^2 - \theta_d^2)}{1 + \theta_d/(3\eta\mu\ell)}. \quad (8)$$

This relation will be used below to study the onset of the transition of the moving liquid drop to a Landau-Levich film.

The dynamical equation [Eq. (5)], which governs the dynamics of the deformation field, can now be written in the linear approximation as

$$\partial_t h(k,t) = -c(v) |k| h(k,t) \quad (9)$$

in Fourier space, where

$$c(v) = \frac{\mu\gamma\theta_d^3(v) - 3\eta\mu\ell v}{3\eta\mu\ell + \theta_d(v)}, \quad (10)$$

with $\theta_d(v)$ to be found by inverting Eq. (8). The corresponding form of the dynamical equation in real space can be found by Fourier transformation as

$$\partial_t h(x,t) = -c(v) \int \frac{dx'}{\pi} \frac{h(x',t)}{(x-x')^2}, \quad (11)$$

which reflects the nonlocality of the dynamics.

Relaxation of the contact line's shape while it is moving thus takes place with the same dispersion relation $\tau^{-1}(k) \sim |k|$ as a contact line at rest, although the corresponding *characteristic velocity* $c(v)$ shows a strong dependence on the contact line velocity v .

IV. CONTACT-ANGLE-VELOCITY RELATION

There can be two types of experiments on a moving contact line depending on how we prepare it. We can fix a value for the contact angle that is different from θ_e , and let it move with an adjusted velocity when it reaches a steady state. This can be achieved, for example, by adding or removing some volume of liquid through a syringe that is inserted in a liquid drop at equilibrium. On the contrary, we can fix the velocity and let the contact angle adjust itself in a steady state. This will be the case, for example, when a plate is withdrawn vertically from a liquid at a constant velocity.

Depending on which “ensemble” we are using, we will have a fixed value for v or θ_d , and we should then use Eq. (8) (that relates the velocity and the dynamic contact angle) to determine the conjugate parameter. The term “ensemble” is in fact quite appropriate to use here because the two (mechanically) conjugate quantities are, in fact, velocity and force, which is determined solely by the contact angle. What we have is then either a “constant velocity” or a “constant force” experiment. It is interesting to note that in nonequilibrium systems, in general, different ensembles may not necessarily lead to the same result [14].

In this work, we are mostly interested in constant velocity experiments, and thus we will treat v as a fixed and given parameter below unless otherwise specified. We will examine Eq. (8) in the limiting cases corresponding to the two different dissipation mechanisms and compare their predictions.

A. Blake approach

The behavior in this regime can be extracted from Eq. (8) by taking the limit $\mu\eta \ll \theta_d$. Inverting the resulting equation yields

$$\left. \frac{\theta_d(v)}{\theta_e} \right|_l = \sqrt{1 - \frac{2v}{c_{l0}}}, \quad (12)$$

in which $c_{l0} = \mu\gamma\theta_e^2$. Note that this holds only for $v < c_{l0}/2$, while $\theta_d = 0$ identically for $v > c_{l0}/2$. This function is plotted in Fig. 2.

As can be readily seen from Fig. 2, increasing v would lead to decreasing values of θ_d until at a critical velocity $v_{lc} = c_{l0}/2$ it finally vanishes continuously. A vanishing con-

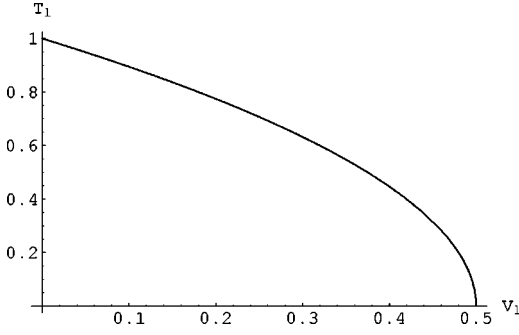


FIG. 2. The reduced order parameter $T_l = (\theta_d / \theta_e)_l$ as a function of the dimensionless velocity $V_l = v / c_{l0}$ for Blake mechanism [Eq. (12)]. The dynamical phase transition at $V_{lc} = 1/2$ is predicted to be of second order in this picture.

tact angle presumably corresponds to formation of a liquid film, a so-called Landau-Levich film. The value of the dynamic contact angle θ_d serves as the order parameter for this dynamical phase transition, while v is the tuning parameter. The continuous vanishing of the order parameter causes the phase transition to be classified as second order. As in the general theory of critical phenomena, a mean-field exponent $\beta = \frac{1}{2}$ is characterizing the vanishing of the order parameter in terms of the tuning parameter.

B. de Gennes approach

In the opposite limit of $\mu \eta \gg \theta_d$, only the hydrodynamic contribution survives, and Eq. (8) leads to

$$\frac{\theta_d(v)}{\theta_e} \Big|_h = \frac{1}{\sqrt{3}} [(-\nu - i\sqrt{1-\nu^2})^{1/3} + (-\nu + i\sqrt{1-\nu^2})^{1/3}], \quad (13)$$

in which $\nu = 3\sqrt{3}v/c_{h0}$ and $c_{h0} = \gamma\theta_e^3/(3\eta\ell)$.¹

The above formula, which holds only for $v < c_{h0}/(3\sqrt{3})$, has two branches and only the one that recovers $\theta_d(0) = \theta_e$ is acceptable as plotted in Fig. 3. While at $v = c_{h0}/(3\sqrt{3})$ we find $\theta_d = \theta_e/\sqrt{3}$, we expect to have $\theta_d = 0$ for higher velocities $v > c_{h0}/(3\sqrt{3})$. Therefore, the order parameter θ_d experiences a finite jump at the transition velocity $v_{hc} = c_{h0}/(3\sqrt{3})$, which is the hallmark of a first-order phase transition.

V. CHARACTERISTIC VELOCITY

Using Eq. (10) and $\theta_d(v)$ that we have found in the preceding section for the two different cases, we can extract the v dependence of the characteristic velocity.

A. Blake approach

We can simplify Eq. (10) by taking the limit $\mu \eta \ll \theta_d$, as

$$c_l(\theta) = c_{l0} \frac{\theta_d^2}{\theta_e^2}. \quad (14)$$

¹Note that the expression in Eq. (13) is real, and the i is retained only to keep the appearance of the formula simpler.

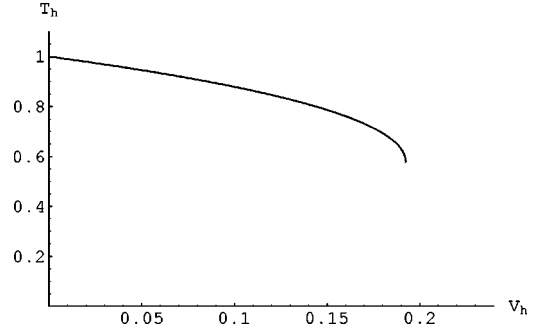


FIG. 3. The reduced order parameter $T_h = (\theta_d / \theta_e)_h$ as a function of the dimensionless velocity $V_h = v / c_{h0}$ for the de Gennes mechanism [Eq. (13)]. The dynamical phase transition at $V_{hc} = 1/(3\sqrt{3}) \approx 0.192$ is predicted to be of first order in this picture.

Inserting the form of $\theta_d(v)$ from Eq. (12) yields

$$c_l(v) = c_{l0} - 2v. \quad (15)$$

Note that in this approach $c(v)$ is strictly linear in v all the way, and it vanishes at the transition point, as plotted in Fig. 4.

B. de Gennes approach

In the opposite limit of $\mu \eta \gg \theta_d$, Eq. (10) will be simplified as

$$c_h(\theta) = \frac{c_{h0}}{2} \left(3 \frac{\theta_d^3}{\theta_e^3} - \frac{\theta_d}{\theta_e} \right). \quad (16)$$

Putting in $\theta_d(v)$ from Eq. (13) leads to

$$c_h(v) = \frac{c_{h0}}{\sqrt{3}} [(-\nu - i\sqrt{1-\nu^2})^{1/3} + (-\nu + i\sqrt{1-\nu^2})^{1/3} - \nu]. \quad (17)$$

One can again check from this equation that $c(v)$ vanishes at the transition. The above equation is plotted in Fig. 5.

The characteristic velocity can be well approximated by the linear expression

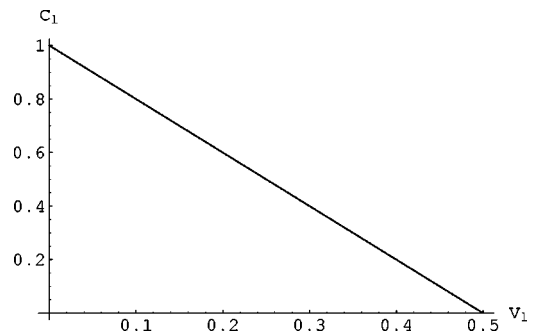


FIG. 4. The reduced characteristic velocity $C_l = c_l / c_{l0}$ as a function of the dimensionless velocity $V_l = v / c_{l0}$ for Blake mechanism [Eq. (15)]. The slope of the curve is -2 all the way to the transition point where the characteristic velocity vanishes.

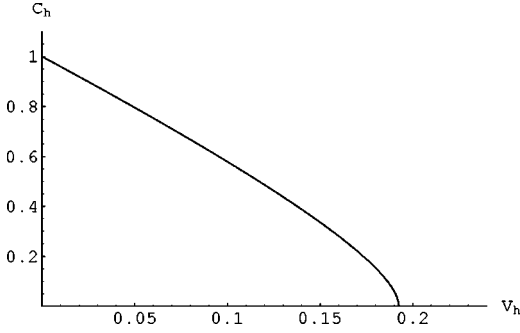


FIG. 5. The reduced characteristic velocity $C_h = c_h/c_{h0}$ as a function of the dimensionless velocity $V_h = v/c_{h0}$ for the de Gennes mechanism [Eq. (17)]. The slope of the curve is nearly -4 until a square-root singularity sets in near the transition point where the characteristic velocity vanishes.

$$c_h(v) \approx c_{h0} - 4v \quad (18)$$

for a wide range of v , except very near $c_{h0}/(3\sqrt{3})$, where it experiences a square-root singular behavior as

$$c_h(v) \approx c_{h0} \left[\sqrt{2} \left(\frac{1}{3\sqrt{3}} - \frac{v}{c_{h0}} \right)^{1/2} + 3 \left(\frac{1}{3\sqrt{3}} - \frac{v}{c_{h0}} \right) + O \left(\left(\frac{1}{3\sqrt{3}} - \frac{v}{c_{h0}} \right)^{3/2} \right) \right]. \quad (19)$$

It is interesting to note that although both approaches predict a sizeable linear regime for $c(v)$, as manifest in Eqs. (15) and (18), the corresponding slopes are predicted differently.

VI. SURFACE DISORDER

In most practical cases, the dynamics of a contact line is affected by the defects and heterogeneities in the substrate, in addition to dissipation and elasticity that we have considered so far. If the interfacial energies γ_{SV} and γ_{SL} are space-dependent with the corresponding averages being $\bar{\gamma}_{SV}$ and $\bar{\gamma}_{SL}$, a displacement $\delta y(x, t)$ of the contact line is going to lead to a change in energy as

$$\delta E_d = \int dx g(x, vt + h(x, t)) \delta y(x, t), \quad (20)$$

where

$$g(x, y) = \gamma_{SV}(x, y) - \gamma_{SL}(x, y) - (\bar{\gamma}_{SV} - \bar{\gamma}_{SL}). \quad (21)$$

Incorporating this contribution in the force balance leads to an extra force term $g(x, vt)$ on the right-hand side of Eq. (5), and thus a noise term on the right-hand side of Eq. (11) of the form

$$\eta(x, t) = \left(\frac{\mu \theta_d}{\theta_d + 3 \eta \mu \ell} \right) g(x, vt), \quad (22)$$

to the leading order. Note that this is a good approximation provided we are well away from the depinning transition, and the contact line is moving fast enough [1,9,12,16].

Assuming that the surface disorder has short-range correlations with a Gaussian distribution described by

$$\langle g(x, y) \rangle = 0,$$

$$\langle g(x, y) g(x', y') \rangle = g^2 a^2 \delta(x - x') \delta(y - y'), \quad (23)$$

we can deduce the distribution of the noise as

$$\langle \eta(x, t) \rangle = 0,$$

$$\langle \eta(x, t) \eta(x', t') \rangle = 2D(v) \delta(x - x') \delta(t - t'), \quad (24)$$

where

$$D(v) = \frac{g^2 a^2}{2v} \left(\frac{\mu \theta_d(v)}{\theta_d(v) + 3 \eta \mu \ell} \right)^2. \quad (25)$$

In the presence of the noise, the contact line undergoes dynamical fluctuations. These fluctuations can best be characterized by the width of the contact line, which is defined as

$$W^2(L, t) \equiv \frac{1}{L} \int dx \langle h(x, t)^2 \rangle. \quad (26)$$

Using Eq. (9) with the noise term, we can calculate the width of the contact line as

$$\begin{aligned} W^2(L, t) &= \frac{D(v)}{\pi c(v)} \int_{\pi/L}^{\pi/a} \frac{dk}{k} [1 - e^{-2c(v)|k|t}] \\ &= \frac{D(v)}{\pi c(v)} \begin{cases} \ln[c(v)t/a], & \frac{a}{c(v)} \ll t \ll \frac{L}{c(v)}, \\ \ln(L/a), & t \gg \frac{L}{c(v)}. \end{cases} \end{aligned} \quad (27)$$

Similarly, we can study the fluctuations in the order-parameter field $\delta \theta(x, t) = \theta(x, t) - \theta_d$. Using Eqs. (7) and (9), we find

$$\begin{aligned} \langle \delta \theta(x, t)^2 \rangle &= \frac{D(v) \theta_d^2(v)}{\pi c(v)} \int_{\pi/L}^{\pi/a} dk k [1 - e^{-2c(v)|k|t}] \\ &= \frac{\pi D(v) \theta_d^2(v)}{2c(v) a^2} \left(1 - \frac{a^2}{2\pi^2 c^2(v) t^2} \right) \end{aligned} \quad (28)$$

for $t \gg a/c(v)$.

The magnitude of the fluctuations of the contact line width

$$\Delta(v) = \frac{D(v)}{\pi c(v)} \quad (29)$$

and, correspondingly, that of the order parameter

$$\sigma(v) = \frac{\pi D(v) \theta_d^2(v)}{2c(v) a^2}, \quad (30)$$

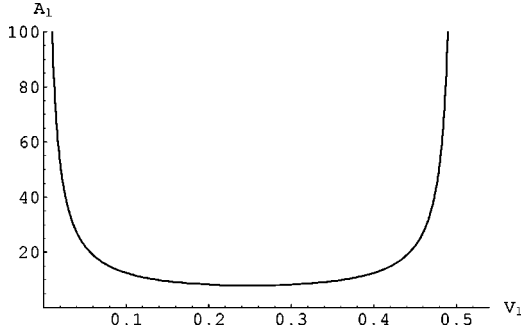


FIG. 6. The reduced width $A_l = \Delta_l / (\mu^2 g^2 a^2 / 2\pi c_{l0}^2)$ as a function of the dimensionless velocity $V_l = v/c_{l0}$ for Blake mechanism [Eq. (31)]. It is symmetric with respect to $V_l = \frac{1}{4}$.

are thus both velocity-dependent. Again, we expect this dependence to be different for the two cases.

A. Blake approach

In this case, we have $\mu\eta \ll \theta_d$, which together with Eqs. (12), (15), (25), (29), and (30) yield

$$\Delta_l(v) = \left(\frac{\mu^2 g^2 a^2}{2\pi c_{l0}^2} \right) \frac{1}{(v/c_{l0})(1-2v/c_{l0})} \quad (31)$$

and

$$\sigma_l(v) = \left(\frac{\pi\mu^2 g^2 \theta_e^2}{4c_{l0}^2} \right) \frac{1}{(v/c_{l0})}. \quad (32)$$

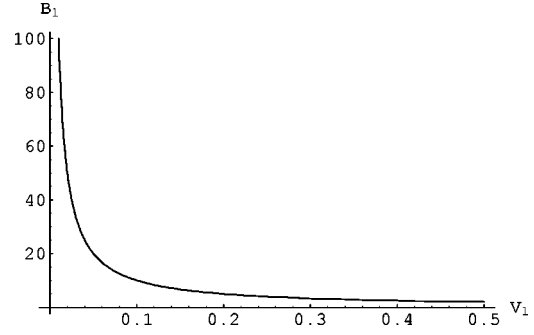


FIG. 7. The reduced order-parameter fluctuations $B_l = \sigma_l / (\pi\mu^2 g^2 \theta_e^2 / 4c_{l0}^2)$ as a function of the dimensionless velocity $V_l = v/c_{l0}$ for the Blake mechanism [Eq. (32)]. It is a monotonically decreasing function of velocity. Note the unusual feature that the order-parameter fluctuations *remain finite* at the transition point, unlike traditional second-order phase transitions.

The above equations are plotted in Figs. 6 and 7. Figure 6 shows that the width of the contact line is a symmetric function of velocity in this picture, while Fig. 7 denotes that the order-parameter fluctuations decrease monotonically with velocity. Note also that these fluctuations remain finite at the transition point, which is not typical of second-order phase transitions.

B. de Gennes approach

Taking the opposite limit $\mu\eta \gg \theta_d$ in Eq. (25), together with Eqs. (13), (17), (29), and (30), we obtain

$$\Delta_h(v) = \left(\frac{g^2 a^2 \theta_e^2}{6\pi\eta^2 \ell^2 c_{h0}^2} \right) \left\{ \frac{[(-\nu - i\sqrt{1-\nu^2})^{1/3} + (-\nu + i\sqrt{1-\nu^2})^{1/3}]^2}{\nu[(-\nu - i\sqrt{1-\nu^2})^{1/3} + (-\nu + i\sqrt{1-\nu^2})^{1/3} - \nu]} \right\} \quad (33)$$

and

$$\sigma_h(v) = \left(\frac{\pi g^2 \theta_e^4}{36\eta^2 \ell^2 c_{h0}^2} \right) \left\{ \frac{[(-\nu - i\sqrt{1-\nu^2})^{1/3} + (-\nu + i\sqrt{1-\nu^2})^{1/3}]^4}{\nu[(-\nu - i\sqrt{1-\nu^2})^{1/3} + (-\nu + i\sqrt{1-\nu^2})^{1/3} - \nu]} \right\}. \quad (34)$$

The above equations are plotted in Figs. 8 and 9. Figure 8 shows that the width of the contact line is not a symmetric function of velocity in this case. Moreover, the order-parameter fluctuations do not decrease monotonically with velocity as shown in Fig. 9. Unlike in the previous case, these fluctuations diverge at the transition point, which is again not typical of first-order phase transitions.

VII. DISCUSSION

Because of their anomalous elasticity, contact lines relax to their equilibrium from an initially distorted configuration with a characteristic inverse decay time $\tau^{-1}(k) = c(v)|k|$ for each k mode. The v dependence of the characteristic velocity

$c(v)$ is shown to depend crucially on the dissipation mechanism, and it can thus be used as an experimental probe for the dominant dissipation mechanism.

A typical experiment for such investigations is direct monitoring of the contact line shape during the relaxation process. If the initial distortion of the contact line can be made periodic in a controlled way, like in the experiment of Ondarcuhu and Veyssie [11], one can directly map out $c(v)$ and hence determine the dissipation mechanism from its v dependence.

Another possibility is to have relaxation from random initial distortions, which will be the case when we pull out a naturally rough plate from the liquid. Monitoring the dynamics of the contact line in this case will provide statistical

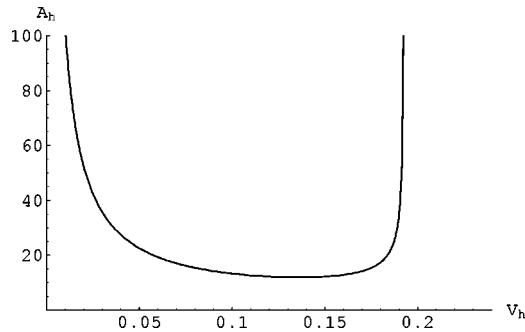


FIG. 8. The reduced width $A_h = \Delta_h / (g^2 a^2 \theta_e^2 / 18 \pi \eta^2 \ell^2 c_{h0}^2)$ as a function of the dimensionless velocity $V_h = v / c_{h0}$ for the de Gennes mechanism [Eq. (33)]. Note the asymmetry of the plot in this case.

information about the relaxation process, from which one can hope to deduce the relevant features discussed in Sec. VI.

We finally note that this linear theory is not sufficient for a complete understanding of the Landau-Levich phase transition, and it breaks down upon approaching the transition point. This breakdown is particularly manifest in the divergence that we encountered in the width of the contact line at the transition point. To be able to have a complete description, one should keep the relevant nonlinear terms that can be calculated by extending the method of this paper, and resort to perturbative renormalization-group approaches for the resulting nonlinear stochastic equation. We have performed these studies, and the corresponding results will appear elsewhere [15].

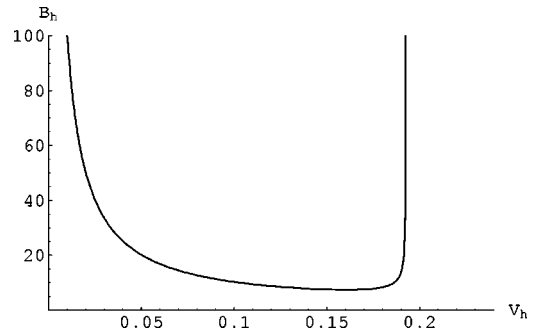


FIG. 9. The reduced order-parameter fluctuations $B_h = \sigma_h / (\pi g^2 \theta_e^4 / 36 \eta^2 \ell^2 c_{h0}^2)$ as a function of the dimensionless velocity $V_h = v / c_{h0}$ for the de Gennes mechanism [Eq. (34)]. In this case, it is *not* a monotonically decreasing function of velocity. Note the unusual feature that the order parameter fluctuations *diverge* at the transition point, unlike traditional first-order phase transitions.

In conclusion, we have studied the relaxation dynamics of the contact lines, and suggested that monitoring this dynamics can provide an experimental probe for the debated dominant dissipation mechanism.

ACKNOWLEDGMENTS

We are grateful to J. Bico, P. G. de Gennes, and D. Quéré for invaluable discussions and comments. One of us (R.G.) would like to thank the group of Professor de Gennes at College de France for their hospitality and support during his visit. This research was supported in part by the National Science Foundation under Grant No. DMR-98-05833 (R.G.).

-
- [1] P.G. de Gennes, *Rev. Mod. Phys.* **57**, 827 (1985).
[2] F. Brochard-Wyart and P.G. de Gennes, *Adv. Colloid Interface Sci.* **39**, 1 (1992).
[3] G. Yarnold and B. Manson, *Proc. Phys. Soc. London, Sect. B* **62**, 121 (1949); **62**, 125 (1949).
[4] T.D. Blake and J.M. Haynes, *J. Colloid Interface Sci.* **30**, 421 (1969); T.D. Blake and K.J. Ruschak, *Nature (London)* **282**, 489 (1979); T. Blake, in *Wettability*, edited by J. Berg (Marcel Dekker, New York, 1993), p. 251.
[5] P.G. de Gennes, *Colloid Polym. Sci.* **264**, 463 (1986); in *Physics of Amphiphilic Layers*, edited by J. Meunier, D. Langevin, and N. Boccardo (Springer, Berlin, 1987); F. Brochard-Wyart, J.M. di Meglio, and D. Quéré, *C. R. Acad. Sci., Ser. II: Mec., Phys., Chim., Sci. Terre Univers* **304**, 553 (1987).
[6] L. Landau and B. Levich, *Acta Physicochim. URSS* **17**, 42 (1942); B. Levich, *Physicochemical Hydrodynamics* (Prentice-Hall, London, 1962).
[7] See also O.V. Voinov, *Fluid Dyn.* **11**, 714 (1976); R.G. Cox, *J. Fluid Mech.* **168**, 169 (1986).
[8] D. Quéré (private communication).
[9] J.F. Joanny and P.G. de Gennes, *J. Chem. Phys.* **81**, 552 (1984).
[10] P.G. de Gennes, *C. R. Acad. Sci., Ser. II: Mec., Phys., Chim., Sci. Terre Univers* **302**, 731 (1986).
[11] T. Ondarcuhu and M. Veyssie, *Nature (London)* **352**, 418 (1991).
[12] For a discussion of the depinning transition in contact lines, see E. Raphaël and P.G. de Gennes, *J. Chem. Phys.* **90**, 7577 (1989); J.F. Joanny and M.O. Robbins, *ibid.* **92**, 3206 (1990); D. Ertas and M. Kardar, *Phys. Rev. E* **49**, R2532 (1994); E. Schäffer and P. Wong, *Phys. Rev. Lett.* **80**, 3069 (1998); *Phys. Rev. E* **61**, 5257 (2000); C. Guthmann, R. Gombrowicz, V. Repain, and E. Rolley, *Phys. Rev. Lett.* **80**, 2865 (1998); A. Hazareesing and M. Mezard, *Phys. Rev. E* **60**, 1269 (1999).
[13] C. Huh and L. Scriven, *J. Colloid Interface Sci.* **35**, 85 (1971).
[14] For an example of different behavior of constant-force and constant-velocity ensembles in wetting systems, see E. Raphaël and P.G. de Gennes, *J. Chem. Phys.* **90**, 7577 (1989); J.F. Joanny and M.O. Robbins, *ibid.* **92**, 3206 (1990).
[15] R. Golestanian and E. Raphaël, *Europhys. Lett.* **55**, 228 (2001).
[16] M.O. Robbins and J.F. Joanny, *Europhys. Lett.* **3**, 729 (1987).